Clumping factor B promotes adherence of Staphylococcus aureus to corneocytes in atopic dermatitis

Fleury, Orla M.; McAleer, Maeve A.; Feuillie, Cécile; Formosa-Dague, Cécile; Sansevere, Emily; Bennett, Désirée E.; Towell, Aisling M.; McLean, W. H. Irwin; Kezic, Sanja; Robinson, D. Ashley; Fallon, Padraic G.; Foster, Timothy J.; Dufrêne, Yves F.; Irvine, Alan D.; Geoghegan, Joan A.

Published in:
Infection and Immunity

DOI:
10.1128/IAI.00994-16

Publication date:
2017

Document Version
Peer reviewed version

Clumping factor B promotes adherence of *Staphylococcus aureus* to corneocytes in atopic dermatitis

Orla M. Fleury*[1], Maeve A. McAleer*[2,3,4], Cécile Feuillie[5], Cécile Formosa-Dague[5], Emily Sansevere[6], Désirée E. Bennett[7], Aisling M. Towell[1], WH Irwin McLean[8], Sanja Kezic[9], D. Ashley Robinson[6], Padraic G. Fallon[2,3], Timothy J. Foster[1], Yves F. Dufrêne[5,10], Alan D. Irvine**[2,3,4], Joan A. Geoghegan**[1]

[1]Department of Microbiology, Moyne Institute of Preventive Medicine, School of Genetics and Microbiology, Trinity College Dublin, Ireland

[2]Clinical Medicine, Trinity College Dublin, Ireland

[3]National Children's Research Centre, Our Lady's Children's Hospital Crumlin, Dublin, Ireland

[4]Paediatric Dermatology, Our Lady's Children's Hospital Crumlin, Dublin, Ireland

[5]Institute of Life Sciences, Université catholique de Louvain, Croix du Sud, 4-5, bte L7.07.06, B-1348 Louvain-la-Neuve, Belgium

[6]Department of Microbiology and Immunology, University of Mississippi Medical Center, Jackson, MS 39216, USA

[7]Epidemiology and Molecular Biology Unit, Temple Street Children's University Hospital, Dublin, Ireland

[8]Dermatology and Genetic Medicine, University of Dundee, UK

[9]Coronel Institute of Occupational Health, Academic Medical Center, Amsterdam, The Netherlands

[10]Walloon Excellence in Life sciences and Biotechnology (WELBIO), Belgium

*, ** equal contributions

[#]Corresponding author: E-mail: geoghegj@tcd.ie. Telephone: +35318961188. Fax: +35316799294

Running Title: ClfB-mediated adherence of *S. aureus* to corneocytes from AD

Abstract

Staphylococcus aureus skin infection is a frequent and recurrent problem in children with the common inflammatory skin disease atopic dermatitis (AD). *S. aureus* colonises the skin of the majority of children with AD and exacerbates the disease. The first step during colonisation and infection is bacterial adhesion to the cornified envelope of corneocytes in the outer layer stratum corneum. Corneocytes from AD skin are structurally different to corneocytes from normal healthy skin. The objective of this study was to identify bacterial proteins that promote the adherence of *S. aureus* to AD corneocytes. *S. aureus* strains from clonal complex 1 and 8 were more frequently isolated from infected AD skin than from the nasal cavity of healthy children. AD strains had increased ClfB ligand binding activity compared to normal nasal carriage strains. Adherence of single *S. aureus* bacteria to corneocytes from AD patients *ex vivo* was studied using atomic force microscopy. Bacteria expressing ClfB recognised ligands distributed over the entire corneocyte surface. The ability of an isogenic ClfB-deficient mutant to adhere to AD corneocytes was greatly reduced compared to its parent clonal complex 1 clinical strain. ClfB from clonal complex 1 strains had a slightly higher binding affinity for its ligand compared to ClfB from other clonal complexes. Our results provide new insights into the first step in the establishment of *S. aureus* colonisation in AD patients. ClfB is a key adhesion molecule for the interaction of *S.aureus* with AD corneocytes and represents a target for intervention.

Introduction

The skin of the majority of individuals with the inflammatory skin disease atopic dermatitis (AD) is heavily colonised by *Staphylococcus aureus* (1). The healthy population has a much lower rate of persistent carriage (~ 20%) and colonisation is usually confined to the nasal cavity (2). *S. aureus* colonization of skin appears to post-date the development of AD, at least in infant populations (3). In established AD the density of *S. aureus* on lesional and non-lesional skin has a strong relationship to disease severity (4). A major risk factor for the development of AD is loss-of-function mutations in the filaggrin (*FLG*) gene (5, 6) which lead to a reduced level of natural moisturising factor (NMF) in the stratum corneum accompanied by a skin epidermal barrier defect and an elevated pH (7). When the skin barrier is compromised, factors produced by *S. aureus* exacerbate the symptoms of AD (8). Several *S. aureus* factors have been linked to increased inflammation and disease severity in AD including α-toxin (9), the staphylococcal superantigens (10) and δ-toxin (11).

S. aureus adheres to the cornified envelope of corneocytes in the stratum corneum. Corneocytes from AD skin have an altered surface topology compared to corneocytes from normal healthy skin, physical characteristics that are largely determined by levels of expressed filaggrin and NMF (12). The factors promoting colonisation of atopic skin have not yet been identified. Several *S. aureus* proteins are known to bind to host molecules, some of which may be present on the surface of the stratum corneum of AD skin. For example, compared with healthy skin, higher levels of fibronectin are found in the stratum corneum of patients with AD and the expression of the *S. aureus* cell wall anchored (CWA) fibronectin binding proteins (FnBPs) A and B enhances bacterial adherence to AD skin biopsy sections (13). The CWA protein clumping factor B (ClfB) binds to the cornified envelope proteins loricrin and cytokeratin 10 in the moist squamous epithelium promoting colonization of the

anterior nares (14, 15). ClfB and FnBPs are expressed at higher levels by bacteria grown *in vitro* at the pH of AD skin than by bacteria grown at the low pH typical of healthy skin (16). The binding of ClfB to its ligands is well understood at the molecular level. The X-ray crystal structure of the ligand-binding region of ClfB has been solved both in the apo form and with a peptide ligand bound (17). Binding occurs by the 'dock, lock and latch' mechanism whereby a short peptide from loricrin or cytokeratin 10 binds to a hydrophobic trench located between the separately folded N2 and N3 subdomains (18). A conformational change at the C-terminus of N3 locks the ligand in place.

The aim of our study was to identify the bacterial factors that promote adherence of *S. aureus* to corneocytes from AD skin. We studied clinically relevant strains of *S. aureus* from the infected lesional skin of children with AD. Molecular typing methods revealed the population structure of strains of *S. aureus* from AD skin infection and *in vitro* experiments demonstrated that AD strains adhere more strongly to a ClfB ligand (the loricrin-derived peptide L2v) than control strains of *S. aureus* isolated from the nares of a healthy cohort of children with no history of AD. Isogenic *clfB* knockout mutants were generated in AD strains representing the most common lineages of *S. aureus* isolated from paediatric patients. The ability of an AD strain and its isogenic ClfB-deficient mutant to adhere to corneocytes from patients with AD was studied *ex vivo* and using atomic force microscopy (19).

Materials and Methods

Patient populations

The AD patients enrolled in this study were presenting for the first time at a tertiary referral centre at Our Lady's Children's Hospital, Crumlin, Dublin, Ireland between September 2012 and September 2014. An experienced paediatric dermatologist (MAMcA ADI, or both) made the diagnosis and recorded the disease phenotype. All patients met the United Kingdom diagnostic criteria for AD (20) and had moderate or severe disease. Exclusion criteria from the study included patients who had pyrexial illness in the preceding 2 weeks and those who had received immunosuppressive systemic therapy, such as oral corticosteroids, in the preceding 3 months. The study was conducted in accordance with the Helsinki Declarations and was approved by the Research Ethics Committee of Our Lady's Children's Hospital, Dublin, Ireland. Full written informed consent was obtained from all patients' parents. The children were treatment naive (for topical steroids, antibiotics or antimicrobials) at presentation. Patient demographics and disease characteristics are summarized in Table S1.

Age-matched control subjects were children attending the Emergency Department of Temple Street Children's University Hospital, Dublin, Ireland between July and August 2009. Subjects were requested to complete a questionnaire and those whose reason for presentation was not of an infective origin (i.e. trauma, accompanying sibling, etc.) and who had no history of skin diseases (including AD), allergic rhinitis or bronchial asthma were selected for inclusion in the study. Ethical permission was received from the Temple Street Children's University Hospital Ethics Committee and full written informed consent was obtained from all patients' parents. The mean age at recruitment was 30.48 months, and 53.06% of the subjects were female.

120

121 **_FLG_ genotyping**

122 All AD patients were screened for the 9 most common *FLG* mutations found in the Irish
123 population (R501X, Y2092X, 2282del4, R2447X, S3247X, R3419X, 3702delG, S1040X,
124 and G1139X) from DNA extracted from a blood sample. The methods used have been
125 previously described (21).

126

127 **Collection of strains and molecular typing of *S. aureus***

128 To collect AD strains, swabs were taken from a clinically infected site on the patient's skin
129 (Table S1) and streaked onto mannitol salt agar to select for *S. aureus*. *S. aureus* strains from
130 a healthy cohort (children with no history of AD and asymptomatic nasal carriage) were
131 recovered by rotational swabbing of the anterior nares of one nostril. In total 44 AD strains
132 and 49 nasal carriage isolates were studied. Strains were single colony purified on sheep
133 blood agar and a single colony isolated from each patient was *spa* typed. The *spa* types were
134 classified using two online nomenclature systems (Ridom and eGenomics) (22). One or more
135 isolates of each unique *spa* type were subjected to multilocus sequence typing (MLST), and
136 clonal complex (CC) was assigned by eBURST analysis of the MLST data.

137

138 **Bacterial growth conditions and strain construction**

139 *S. aureus* was grown in Tryptic Soy Broth (TSB) at 37°C. SH1000 is a commonly used
140 laboratory strain of *S. aureus* (23). Plasmid DNA isolated from *E. coli* strain SA08B (24)
141 was used to transform CC1 strains of *S. aureus* using standard procedures (25). Deletion of

142 the *clfB* gene was achieved by allelic exchange as described previously (14). The mutation
143 was confirmed by DNA sequencing of a PCR amplimer. The *clfB* mutant was phenotypically
144 indistinguishable from the parent strain in terms of growth rate and haemolysis on sheep
145 blood agar (data not shown). Plasmids pCU1 (26) and pCU1::*clfB* (27) were transformed
146 into AD08$_{CC1}$Δ*clfB*.

147

148 **Extraction of cell wall proteins and western immunoblotting**

149 Bacteria from an overnight culture were washed in TSB, diluted 1:200 and allowed to grow
150 to an OD_{600} = 0.3 - 0.5 in TSB. Bacteria were washed in phosphate-buffered saline (PBS)
151 and resuspended to an OD_{600} of 10 in lysis buffer (50 mM Tris/HCl, 20 mM $MgCl_2$, pH 7.5)
152 supplemented with raffinose (30% w/v, Sigma) and complete protease inhibitors (40 µl/ml,
153 Roche). Cell wall proteins were solubilised by incubation with lysostaphin (100 µg/ml;
154 AMBI, New York) for 8 min at 37°C. Protoplasts were removed by centrifugation at
155 16,000 × *g* for 5 min and the supernatant containing solubilised cell wall proteins was
156 aspirated and boiled for 10 min in final sample buffer. Proteins were separated by sodium
157 dodecyl sulfate polyacrylamide gel electrophoresis on 7.5% (w/v) polyacrylamide gels,
158 transferred onto polyvinylidene difluoride (Roche) and blocked in 10% (w/v) skimmed milk
159 proteins. Blots were probed with polyclonal rabbit antibodies against the ClfB A domain
160 (1:1000) and bound antibody was detected using horseradish peroxidise-conjugated protein A
161 (1:500, Sigma). Reactive bands were visualised using the LumiGLO reagent and peroxide
162 detection system (Cell Signalling Technology) using the ImageQuant Las 4000 imaging
163 system and ImageQuant TL software (GE Healthcare).

164

165 **Bacterial adherence to L2v**

Recombinant GST-tagged L2v was purified from *E. coli* as previously described (14) using a GSTrap FF purification column (GE Healthcare) according to the manufacturer's instructions and diluted in coating buffer (0.1 M $NaHCO_3$, 33 mM Na_2CO_3, pH 9.6). Wells of a microtitre plate (Nunc maxisorb) were incubated with a solution of L2v (0.625 µg/ml) overnight at 4°C. Wells were blocked with bovine serum albumin (BSA, 5% (w/v)) for 2 h at 37°C. *S. aureus* was grown to an OD_{600} = 0.3 - 0.5 in TSB. Washed bacteria were adjusted to an OD_{600} of 1.0 in PBS, and 100 µl was added to each well and incubated for 1.5 h at 37 °C. Wells were washed with PBS, and adherent cells fixed with formaldehyde (25% v/v), stained with crystal violet and the A570 nm measured. Each experiment was performed three times.

Sampling of the stratum corneum by tape stripping and transepidermal water loss measurement

A clinically unaffected site on the patient's volar forearm was used for transepidermal water loss (TEWL) measurements and stratum corneum sampling using a previously described method (28). TEWL was determined by using a Tewameter 300 (Courage and Khazaka Electronic GmbH, Cologne, Germany). To sample the stratum corneum, circular adhesive tape strips (3.8 cm^2, D-Squame; Monaderm, Monaco, France) were attached to volar forearm skin and pressed for 10 seconds with a constant pressure (225 g/cm^2) by using a D-Squame Pressure Instrument D500 (CuDerm, Dallas, Tex). The tape strip was then gently removed and placed in a closed vial. Eight consecutive tape strips were sampled, all from the same site. The tape strips were immediately stored at −80°C until analysis. The fifth strip was used for NMF measurements and the eighth strip for AFM.

Natural moisturising factor measurement

Natural moisturising factor analysis was performed on the fifth consecutive strip, according to methods described in detail previously (29). Briefly, the tape strip was extracted with 25% (wt/wt) ammonia solution. After evaporation of the ammonia extract, the residue was dissolved in 250 µl of pure water and analyzed by using high performance liquid chromatography. The NMF concentration was normalized for the protein amount determined with a Pierce Micro BCA protein assay kit (Thermo Fischer Scientific, Rockford, Ill; referred to as the Pierce assay) to compensate for a variable amount of the stratum corneum on the tape.

Atomic Force Microscopy

Corneocyte imaging. Atomic force microscopy imaging was performed on the eighth tape strip in contact mode at a resolution of 512 lines, using $SiNO_3$ cantilevers (MSCT, Bruker, nominal spring constant of 0.01 N/m), in Tris buffered saline (TBS, Tris 50 mM, NaCl 150 mM, pH = 7.4) at room temperature. For each condition, at least 3 different corneocytes were imaged.

Multiparametric imaging. Multiparametric images of corneocytes were recorded in TBS using the Quantitative Imaging™ mode available on the Nanowizard III AFM (JPK Instruments, Germany). Images were obtained using a *S. aureus* $AD08_{CC1}$ or $AD08_{CC1}\Delta$*clfB* cell probe (see below for cell probe preparation) at 128 pixels x 128 pixels, with an applied force kept at 1.0 nN, and a constant approach/retract speed of 40.0 µm/s (z-range of 1 µm). The cantilevers spring constants were determined by the thermal noise method. For each condition, experiments were repeated for at least 3 different cell pairs.

Single-cell force spectroscopy. To prepare bacterial cell probes, colloidal probes were obtained by attaching a single silica microsphere (6.1 µm diameter, Bangs Laboratories) with a thin layer of UV-curable glue (NOA 63, Norland Edmund Optics) on triangular tipless cantilevers (NP-O10, Bruker) and using a Nanowizard III AFM (JPK Instrument, Berlin, Germany). Cantilevers were then immersed for 1 h in TBS (pH = 8.5) containing dopamine hydrochloride (4 mg/ml, Sigma-Aldrich), rinsed in TBS, and used directly for cell probe preparation. The nominal spring constant of the colloidal probe cantilever was determined by the thermal noise method. Then, 50 µl of a diluted cell suspension was deposited into the petri dish containing corneocytes, at a distinct location within the petri dish; 3 ml of PBS was added to the system. The colloidal probe was brought into contact with an isolated bacterium and retracted to attach the bacterial cell; proper attachment of the cell on the colloidal probe was checked using optical microscopy. Cell probes were used to measure cell-cell interaction forces at room temperature, using an applied force of 0.25 nN, a constant approach-retraction speed of 1.0 µm/s and a contact time of 100 ms. Data were analyzed using the Data Processing software from JPK Instruments (Berlin, Germany). Adhesion forces values were obtained by calculating the maximum adhesion force for each force curve recorded on corneocytes and the data for five different cell pairs in each condition were pooled.

Recombinant ClfB protein expression and purification. DNA encoding the N2N3 subdomains of ClfB (residues 201-542) was amplified by PCR using genomic DNA from *S. aureus* strain $AD08_{CC1}$ or $AD22_{CC30}$ as template and cloned into the vector pQE30. *E. coli* TOPP3 carrying the recombinant plasmids was grown to late exponential phase (OD_{600} = 0.6) and induced with IPTG. CC1 and CC30 ClfB harbouring an N-terminal hexahistidine tag were purified using Ni^{2+} affinity chromatography.

Surface plasmon resonance. Surface plasmon resonance (SPR) was performed using the BIAcore X100 system (GE Healthcare). Goat anti-GST IgG (30 µg/ml, GE Healthcare) was

diluted in 10 mM sodium acetate buffer at pH 5.0 and immobilized on CM5 sensor chips using amine coupling. This was performed using 1-ethyl-3-(3-dimethylaminopropyl) carbodiimide hydrochloride, followed by *N*-hydroxysuccinimide and ethanolamine hydrochloride, as described by the manufacturer. Recombinant GST-tagged L2v (10–30 µg/ml) in PBS was passed over the anti-GST surface of one flow cell while recombinant GST (10–30 µg/ml) was passed over the other flow cell to provide a reference surface. Increasing concentrations of rClfB N2N3 in PBS were passed in over the surface of the chip without regeneration. All sensorgram data were subtracted from the corresponding data from the reference flow cell. The response generated from injection of buffer over the chip was also subtracted from each sensorgram. Data was analysed using the BIAevaluation software version 3.0. A plot of the level of binding (response units) at equilibrium against concentration of rClfB N2N3 was used to determine the $K_{D.}$ The data shown is representative of 3 individual experiments.

Statistical Tests

Statistical significance was determined with the Student's *t*-test, using GRAPHPAD software.

Results

Population structure of atopic dermatitis strains of *S. aureus*.

The skin of AD patients is frequently colonised by *S. aureus*. This study aimed to identify bacterial factors that promote adherence of AD strains of *S. aureus* to corneocytes from AD skin. To facilitate this, strains of *S. aureus* were collected from infected skin lesions of children with AD (AD strains). The paediatric patients were presenting for the first time at a tertiary referral centre in Dublin, Ireland and were treatment naïve (Table S1). Molecular typing methods were used to assign each strain to a clonal complex so that the general population structure of the AD strains could be examined. The most common clonal complex (CC) in the AD cohort was CC1 (9 isolates, 20.45%) followed by CC45 (7 isolates, 15.9%), CC8 (6 isolates, 13.63%) and CC5 (6 isolates, 13.63%) (Fig. 1A). Commensal *S. aureus* strains from a healthy cohort in Dublin, Ireland (children with no history of AD and asymptomatic nasal carriage) were also typed to the same level (control strains, Fig. 1B) Only 4.08% and 2.04% of the control strains belonged to CC1 and CC8, respectively, showing that although CC1 and CC8 strains are frequently recovered from AD skin lesions they rarely occur as commensal strains in the nares of healthy children in the community (Fig. 1). In contrast, while CC30 was the most prevalent clonal complex among the control strains (33% of strains) only 6.81% of the AD strains belonged to CC30 showing a statistically significant underrepresentation of CC30 in the AD cohort. Thus the strains causing skin infection in paediatric AD patients are different to the commensal strains circulating in the community. There were no associations between the *S. aureus* clonal complex and NMF levels in the patient's stratum corneum or the clinical phenotype (Table S1).

Ligand binding activity of AD strains.

Disease causing strains of *S. aureus* often have increased ability to adhere to host molecules or increased toxin production compared to commensal strains (30, 31). We hypothesised that adhesion to corneocytes is an important first step in the colonisation and infection of AD skin. Therefore we employed a phenotypic screening method to study the activity of the *S. aureus* adhesin ClfB, a *S. aureus* CWA protein that binds to loricrin and cytokeratin 10 (14, 15). We examined the in vitro adherence of AD strains to the ClfB ligand L2v, a loricrin derived peptide fused to GST (Fig. 2). The well characterised *S. aureus* strain SH1000 was included as a control since adherence of SH1000 to L2v is solely dependent on ClfB (14). The amount of adherence for each clinical strain was expressed as a percentage of the adherence value measured for SH1000. The commensal control strains were also tested. Each data point in Fig. 2 represents the mean adherence level of a single strain. All AD strains adhered to immobilized L2v with a median level of adherence relative to SH1000 of 157% (Fig. 2). The median level of adherence for the control strains was significantly lower (111%, $p < 0.0001$). These results indicate that all *S. aureus* strains that infect the skin of AD patients display ClfB ligand binding activity and that this is higher than the *S. aureus* nasal carriage control isolates from healthy individuals. These data suggested that ClfB could be an important adhesin for AD skin. In addition AD strains from CC1 (red), the most common clonal complex in the AD cohort, adhered very strongly to L2v with a median adherence value of 196% (Fig. 2). For the CC30 strains (green) adherence values ranged between 0 and 155% for the control strains while for the three CC30 AD strains, adherence values ranged between 144 and 191%. Adherence values for the CC8 strains (blue) were highly variable ranging from 41 – 204%.

300

301 **Adherence of *S. aureus* to corneocytes from AD patients *ex vivo* is ClfB-dependent.**

302 The results described above suggested that ClfB ligand binding activity was a universal
303 feature of our paediatric AD strains. In order to investigate if adherence of *S. aureus* to AD
304 corneocytes requires ClfB, the *clfB* gene was deleted in a representative AD strain from CC1
305 ($AD08_{CC1,}$ Table S1). Western immunoblotting using anti-ClfB IgG indicated that while the
306 parent strain AD08 expressed ClfB, bands corresponding to ClfB were not detected for the
307 ClfB-deficient mutant ($AD08_{CC1}\Delta$*clfB*, Fig. 3A). Complementation of the *clfB* mutant with
308 plasmid pCU1::*clfB* restored the expression of ClfB (Fig. 3A). The *clfB* mutant did not
309 adhere to L2v while the parent strain adhered in a dose-dependent and saturable manner (Fig.
310 3B). Complementation of $AD08_{CC1}\Delta$*clfB* with pCU1::*clfB* restored the ability of the mutant
311 to adhere to L2v while $AD08_{CC1}\Delta$*clfB* carrying empty plasmid pCU1 could not adhere (Fig.
312 3C) showing that the ability of $AD08_{CC1}$ to adhere strongly to L2v can be attributed to the
313 activity of ClfB.

314 $AD08_{CC1}$ and its isogenic ClfB-deficient mutant were used in single cell atomic force
315 microscopy (AFM) experiments to determine if ClfB is important for the adherence of *S.*
316 *aureus* to AD skin. Corneocytes were collected by tape-stripping the unaffected skin of two
317 AD patients with low NMF levels and concurrent *S. aureus* infection at a different site
318 (patients 1434 and 1473, Table S1). Previous work has shown that low levels of NMF are
319 associated with changes in corneocyte morphology in AD skin compared to normal healthy
320 skin leading to the appearance of villus-like projections (12). We generated topographic
321 images of corneocytes from both patients in buffer, using contact mode imaging with silicon
322 nitride tips (Fig. S1) and found that the corneocytes from FLG AD patients displayed large

numbers of villus protrusions, about 200 nm in height, consistent with the morphology expected at low NMF (12).

To investigate if ClfB is important for the adherence of *S. aureus* to corneocytes from AD skin, $AD08_{CC1}$ and its isogenic ClfB-deficient mutant ($AD08_{CC1}\Delta$*clfB*) were used in single-cell force spectroscopy experiments (32, 33) (Fig. 4). A single *S. aureus* cell was immobilised on an AFM cantilever and this was used as a probe to measure the binding forces between *S. aureus* adhesins and corneocytes. The average binding force between *S. aureus* $AD08_{CC1}$ and AD corneocytes was similar for both patients (1186 pN and 1109 pN, Fig. 4A). In both cases there was a statistically significant reduction in binding force when $AD08_{CC1}\Delta$*clfB* was used as a probe on the same AD corneocytes (670 pN and 749 pN, Fig. 4C). These data provide direct evidence that ClfB is involved in mediating attachment of *S. aureus* to AD corneocytes.

Multiparametric imaging was then used to localise ligands recognised by *S. aureus* on the surface of corneocytes from patients 1434 and 1473 (34, 35). Multiparametric imaging is a newly developed AFM technique that enables researchers to simultaneously map the structure, biophysical properties and molecular interactions of biological samples (19). AFM cantilevers were functionalised with a single cell of $AD08_{CC1}$ or $AD08_{CC1}\Delta$*clfB*. Force curves were recorded across the corneocyte surface at high frequency, generating maps of structure and adhesion. Multiple adhesion events with a mean force of ,~ 600 pN occurred between $AD08_{CC1}$ and the corneocyte surface indicating that many ligands for *S. aureus* are exposed in the stratum corneum of AD patients (Fig. 5). In contrast, much fewer adhesion events with a weaker strength (~200 pN) occurred with $AD08_{CC1}\Delta$*clfB* indicating that in the absence of ClfB, *S. aureus* is less well able to adhere to corneocytes (Fig. 5). Importantly, the number of ligands supporting *S. aureus* adherence to the surface of corneocytes was greatly reduced for

the ClfB mutant. This demonstrates that ClfB is a major adhesin mediating the interaction of *S. aureus* with AD skin.

Ligand binding by ClfB from AD strains

All AD strains adhered to L2v and the median adherence level was high (Fig. 2B). ClfB is the only S. *aureus* factor that binds to L2v (Fig. 3, (14). Variation in the amino-acid sequence of the ligand binding domains of ClfB has been reported previously (36). More sequence differences in ClfB are likely to occur between clonal complexes of *S. aureus* than within a clonal complex (36). Amino acid sequence variation in ClfB could confer a higher affinity for the ligand. We isolated genomic DNA from all AD strains and used PCR to amplify DNA encoding the ligand binding region of ClfB (N2 and N3 subdomains). All AD strains carried the *clfB* gene (data not shown). DNA sequencing was carried out on the *clfB* amplimer that was generated for all of the CC1, CC8 and CC30 strains. The deduced amino-acid sequences were aligned. The ClfB N2N3 subdomains of CC1 strains shared 100% amino acid identity with each other. The amino acid sequences of ClfBN2N3 from CC8 strains were 92% identical to the CC1 sequence. The three CC30 AD strains had identical ClfBN2N3 sequences that shared 94% identity with CC1 ClfB N2N3. Molecular modelling was carried out to allow visualisation of the position of the variant residues on the crystal structure of ClfB N2N3 (Fig. 6A). This indicated that the residues that vary between CC1 and CC30 are located well away from the trench between N2 and N3. Thus they are unlikely to alter the affinity of ligand binding to the trench by the dock, lock and latch mechanism. However it is possible that an additional, unknown ligand binding site could be located outside of the trench region. For example it has recently been shown for the related protein ClfA that high-affinity binding of ClfA to its ligand fibrinogen involves both the dock, lock and latch ligand-binding trench and a second interaction site at the top of the N3 subdomain

(37). Thus to investigate if sequence differences outside of the trench region in CC1 and CC30 ClfB might alter the affinity for L2v, 6x histidine-tagged recombinant ClfB N2N3 proteins (rClfB N2N3) were purified from *E. coli*. The affinity of rClfB N2N3 with CC1 or CC30 sequence for L2v was studied using surface plasmon resonance. GST-tagged L2v was captured on the surface of a sensor chip that had been coated with anti-GST IgG and increasing concentrations of rClfB N2N3 proteins were passed over the surface of the coated sensor chip. To calculate the K_D the amount of binding at equilibrium was plotted against each rClfB N2N3 concentration and the K_D of the interaction was calculated (Fig. 6). Previously the affinity of CC8 rClfB N2N3 for L2v was calculated to be 2.21 μM (14). CC1 rClfB N2N3 had a slightly higher affinity for GST-L2v (1.91 ± 0.17 μM, Fig. 6B) than CC30 rClfB N2N3 (3.26 ± 0.36 μM, Fig. 6C). The small but statistically significant difference in affinity of CC1 and CC30 ClfB for L2v ($p < 0.001$) may partially explain why AD strains from CC1 adhere more strongly to L2v.

Discussion

The skin of AD patients differs in several respects from normal skin and provides an environment where *S. aureus* can proliferate. By mutating the *clfB* gene we have shown the importance of ClfB in mediating bacterial adherence to corneocytes taken from AD patients known to be susceptible to *S. aureus*. This study used clinically relevant strains isolated from AD patients, rather than relying on laboratory strains, thus increasing the clinical relevance of our findings. Single cell AFM is an important recent technical advance which has allowed measurement of the forces involved in binding of single bacterial cells to corneocytes (34). Here we show that a *clfB* mutant bound significantly less strongly to corneocytes from two AD patients with low NMF compared to the wild-type *S. aureus* parent strain. This demonstrates the importance of ClfB-mediated adherence to ligands exposed on the corneocyte surface. The cornified envelope proteins loricrin and cytokeratin 10 are ligands for ClfB and it may be through binding to these proteins that ClfB mediates bacterial attachment to corneocytes. Alternatively, given the altered corneocyte morphology and protein expression profiles in AD skin, where NMF levels are low (12, 38, 39) it is possible that ClfB is binding to other protein ligands. Additional *S. aureus* factors are likely to contribute to the adhesion of *S. aureus* to corneocytes and colonisation of AD skin. We believe that AFM could be used in future research to gain further insight into the molecular basis of skin colonisation and infection in AD.

There were differences in the overall population structure of *S. aureus* strains from AD skin lesions compared to strains isolated from a control population (commensal strains). This is not entirely surprising given that the niche occupied by the bacteria is very different (AD skin lesion versus nasal cavity). Nevertheless the control strains provided a useful comparison. Since ClfB is a major determinant of nasal colonisation (14) it was surprising to find that ClfB ligand binding activity was lower among commensal control strains compared to AD

strains. However nasal colonisation is a multifactorial process involving several staphylococcal factors (40) and the relative contribution of each factor may differ from strain to strain. We hypothesise that efficient colonisation of AD skin is also likely to require additional factors. Currently there is no explanation as to why there are few CC30 strains isolated from skin lesions in AD patients while the proportion of CC1 and CC8 strains is high. Other studies have found similar trends in AD strain populations from different geographic locations (41, 42). A slightly higher binding affinity was measured for the ClfB from CC1 compared to CC30. We hypothesise that this difference could be amplified when multiple copies of ClfB are present on the surface of *S. aureus* leading to an increase in avidity. In addition it is possible that there are strain-dependent differences in the genetic regulation of *clfB* expression which could account for differences in the amount of ClfB on the surface of different strains. Genetic diversity between strains within a CC can often be missed using molecular typing approaches (43). Whole genome sequencing allows a more detailed analysis of the relationship between strains. It is likely that the ability to colonize and to proliferate on AD skin is due to many factors in addition to the ability to adhere to corneocytes. A detailed proteomic analysis or transcriptional profiling of clinical isolates will give full details of the repertoire of virulence and colonisation factors expressed by strains infecting AD lesions. Here we have identified a crucial role for ClfB in promoting adherence of clinically relevant strains of *S. aureus* to corneocytes from AD skin. This finding advances our understanding of the interaction between *S. aureus* and the altered environment of AD skin and may inform targeted therapies to reduce colonisation and infection in AD patients.

Acknowledgements

OMF, McMcA and ADI are funded by the National Children's Research Centre, Dublin, Ireland. AMT and JAG are supported by a Research Award from the British Skin Foundation. WHIM, PGF and ADI were supported by Wellcome Trust (Programme grant 092530/Z/10/Z). Work at the Université catholique de Louvain was supported by the European Research Council (ERC) under the European Union's Horizon 2020 research and innovation programme (grant agreement No [693630]), the National Fund for Scientific Research (FNRS), the FNRS-WELBIO (Grant n°WELBIO-CR-2015A-05), the Université catholique de Louvain (Fonds Spéciaux de Recherche), the Federal Office for Scientific, Technical and Cultural Affairs (Interuniversity Poles of Attraction Programme), and the Research Department of the Communauté française de Belgique (Concerted Research Action). Y.F.D. and C. F.-D. are respectively Research Director and postdoctoral researcher of the FNRS. D.A.R. was supported by grant GM080602 from the National Institutes of Health. The collection and molecular typing of the carriage isolates was supported by funds from Temple Street Children's University Hospital. We gratefully acknowledge the participation of our patients and their families, without this the study would not have been possible. Many thanks to our research nurse Nuala Alyward for her assistance in sample collection and to Stephanie MacCallum and Linda Campbell for *FLG* genotyping of our patient series.

460 **References**

461 1. **Park HY, Kim CR, Huh IS, Jung MY, Seo EY, Park JH, Lee DY, Yang JM.**
462 2013. *Staphylococcus aureus* Colonization in Acute and Chronic Skin Lesions of
463 Patients with Atopic Dermatitis. Ann Dermatol **25:**410-416.
464 2. **van Belkum A, Verkaik NJ, de Vogel CP, Boelens HA, Verveer J, Nouwen JL,**
465 **Verbrugh HA, Wertheim HF.** 2009. Reclassification of *Staphylococcus aureus*
466 nasal carriage types. J Infect Dis **199:**1820-1826.
467 3. **Kennedy EA, Connolly J, Hourihane JO, Fallon PG, McLean WH, Murray D, Jo**
468 **JH, Segre JA, Kong HH, Irvine AD.** 2017. Skin microbiome before development of
469 atopic dermatitis: Early colonization with commensal staphylococci at 2 months is
470 associated with a lower risk of atopic dermatitis at 1 year. J Allergy Clin Immunol
471 139(1):166-172.
472 4. **Tauber M, Balica S, Hsu CY, Jean-Decoster C, Lauze C, Redoules D, Viode C,**
473 **Schmitt AM, Serre G, Simon M, Paul CF.** 2016. *Staphylococcus aureus* density on
474 lesional and nonlesional skin is strongly associated with disease severity in atopic
475 dermatitis. J Allergy Clin Immunol **137:**1272-1274 e1273.
476 5. **Palmer CN, Irvine AD, Terron-Kwiatkowski A, Zhao Y, Liao H, Lee SP, Goudie**
477 **DR, Sandilands A, Campbell LE, Smith FJ, O'Regan GM, Watson RM, Cecil JE,**
478 **Bale SJ, Compton JG, DiGiovanna JJ, Fleckman P, Lewis-Jones S,**
479 **Arseculeratne G, Sergeant A, Munro CS, El Houate B, McElreavey K, Halkjaer**
480 **LB, Bisgaard H, Mukhopadhyay S, McLean WH.** 2006. Common loss-of-function
481 variants of the epidermal barrier protein filaggrin are a major predisposing factor for
482 atopic dermatitis. Nat Genet **38:**441-446.
483 6. **Irvine AD, McLean WH, Leung DY.** 2011. Filaggrin mutations associated with skin
484 and allergic diseases. N Engl J Med **365:**1315-1327.

7. **McAleer MA, Irvine AD.** 2013. The multifunctional role of filaggrin in allergic skin disease. J Allergy Clin Immunol **131:**280-291.

8. **Kobayashi T, Glatz M, Horiuchi K, Kawasaki H, Akiyama H, Kaplan DH, Kong HH, Amagai M, Nagao K.** 2015. Dysbiosis and *Staphylococcus aureus* Colonization Drives Inflammation in Atopic Dermatitis. Immunity **42:**756-766.

9. **Wichmann K, Uter W, Weiss J, Breuer K, Heratizadeh A, Mai U, Werfel T.** 2009. Isolation of alpha-toxin-producing *Staphylococcus aureus* from the skin of highly sensitized adult patients with severe atopic dermatitis. Br J Dermatol **161:**300-305.

10. **Zollner TM, Wichelhaus TA, Hartung A, Von Mallinckrodt C, Wagner TO, Brade V, Kaufmann R.** 2000. Colonization with superantigen-producing *Staphylococcus aureus* is associated with increased severity of atopic dermatitis. Clin Exp Allergy **30:**994-1000.

11. **Nakamura Y, Oscherwitz J, Cease KB, Chan SM, Munoz-Planillo R, Hasegawa M, Villaruz AE, Cheung GY, McGavin MJ, Travers JB, Otto M, Inohara N, Nunez G.** 2013. Staphylococcus delta-toxin induces allergic skin disease by activating mast cells. Nature **503:**397-401.

12. **Riethmuller C, McAleer MA, Koppes SA, Abdayem R, Franz J, Haftek M, Campbell LE, MacCallum SF, McLean WH, Irvine AD, Kezic S.** 2015. Filaggrin breakdown products determine corneocyte conformation in patients with atopic dermatitis. J Allergy Clin Immunol **136:**1573-1580 e1571-1572.

13. **Cho SH, Strickland I, Boguniewicz M, Leung DY.** 2001. Fibronectin and fibrinogen contribute to the enhanced binding of *Staphylococcus aureus* to atopic skin. J Allergy Clin Immunol **108:**269-274.

14. **Mulcahy ME, Geoghegan JA, Monk IR, O'Keeffe KM, Walsh EJ, Foster TJ, McLoughlin RM.** 2012. Nasal colonisation by *Staphylococcus aureus* depends upon clumping factor B binding to the squamous epithelial cell envelope protein loricrin. PLoS Pathog **8:**e1003092.

15. **O'Brien LM, Walsh EJ, Massey RC, Peacock SJ, Foster TJ.** 2002. *Staphylococcus aureus* clumping factor B (ClfB) promotes adherence to human type I cytokeratin 10: implications for nasal colonization. Cell Microbiol **4:**759-770.

16. **Miajlovic H, Fallon PG, Irvine AD, Foster TJ.** 2010. Effect of filaggrin breakdown products on growth of and protein expression by *Staphylococcus aureus*. J Allergy Clin Immunol **126:**1184-1190 e1183.

17. **Ganesh VK, Barbu EM, Deivanayagam CC, Le B, Anderson AS, Matsuka YV, Lin SL, Foster TJ, Narayana SV, Hook M.** 2011. Structural and biochemical characterization of *Staphylococcus aureus* clumping factor B/ligand interactions. J Biol Chem **286:**25963-25972.

18. **Ponnuraj K, Bowden MG, Davis S, Gurusiddappa S, Moore D, Choe D, Xu Y, Hook M, Narayana SV.** 2003. A "dock, lock, and latch" structural model for a staphylococcal adhesin binding to fibrinogen. Cell **115:**217-228.

19. **Xiao J, Dufrene YF.** 2016. Optical and force nanoscopy in microbiology. Nat Microbiol 1:16186.

20. Williams HC, Burney PG, Hay RJ, Archer CB, Shipley MJ, Hunter JJ, Bingham EA, Finlay AY, Pembroke AC, Graham-Brown RA, Atherton DA, Lewis-Jones MS, Holden CA, Harper JI, Champion RH, Poyner TF, Launer J, David TJ. 1994. The U.K. Working Party's Diagnostic Criteria for Atopic Dermatitis. I. Derivation of a minimum set of discriminators for atopic dermatitis. Br J Dermatol 131:383-396.

21. **Sandilands A, Smith FJ, Irvine AD, McLean WH.** 2007. Filaggrin's fuller figure: a glimpse into the genetic architecture of atopic dermatitis. J Invest Dermatol **127:**1282-1284.

22. **Robinson DA, Enright MC.** 2003. Evolutionary models of the emergence of methicillin-resistant *Staphylococcus aureus*. Antimicrob Agents Chemother **47:**3926-3934.

23. **Horsburgh MJ, Aish JL, White IJ, Shaw L, Lithgow JK, Foster SJ.** 2002. sigmaB modulates virulence determinant expression and stress resistance: characterization of a functional rsbU strain derived from *Staphylococcus aureus* 8325-4. J Bacteriol **184:**5457-5467.

24. **Monk IR, Tree JJ, Howden BP, Stinear TP, Foster TJ.** 2015. Complete Bypass of Restriction Systems for Major *Staphylococcus aureus* Lineages. MBio **6:**e00308-00315.

25. **Lofblom J, Kronqvist N, Uhlen M, Stahl S, Wernerus H.** 2007. Optimization of electroporation-mediated transformation: *Staphylococcus carnosus* as model organism. J Appl Microbiol **102:**736-747.

26. **Augustin J, Rosenstein R, Wieland B, Schneider U, Schnell N, Engelke G, Entian KD, Gotz F.** 1992. Genetic analysis of epidermin biosynthetic genes and epidermin-negative mutants of *Staphylococcus epidermidis*. Eur J Biochem 204:1149-1154.

27. **Ni Eidhin D, Perkins S, Francois P, Vaudaux P, Hook M, Foster TJ.** 1998. Clumping factor B (ClfB), a new surface-located fibrinogen-binding adhesin of *Staphylococcus aureus*. Mol Microbiol **30:**245-257.

28. **Kezic S, O'Regan GM, Lutter R, Jakasa I, Koster ES, Saunders S, Caspers P, Kemperman PM, Puppels GJ, Sandilands A, Chen H, Campbell LE, Kroboth K, Watson R, Fallon PG, McLean WH, Irvine AD.** 2012. Filaggrin loss-of-function

mutations are associated with enhanced expression of IL-1 cytokines in the stratum corneum of patients with atopic dermatitis and in a murine model of filaggrin deficiency. J Allergy Clin Immunol **129:**1031-1039 e1031.

29. **Dapic I, Yau N, Kezic S, Kammeyer A.** 2013. Evaluation of a HPLC method for the determination of natural moisturising factors in the human stratum corneum. Analytical Letters **46:**2133–2144.

30. **Laabei M, Massey R.** 2016. Using functional genomics to decipher the complexity of microbial pathogenicity. Curr Genet **62:**523-525.

31. **Lower SK, Lamlertthon S, Casillas-Ituarte NN, Lins RD, Yongsunthon R, Taylor ES, DiBartola AC, Edmonson C, McIntyre LM, Reller LB, Que YA, Ros R, Lower BH, Fowler VG, Jr.** 2011. Polymorphisms in fibronectin binding protein A of *Staphylococcus aureus* are associated with infection of cardiovascular devices. Proc Natl Acad Sci U S A **108:**18372-18377.

32. **Beaussart A, El-Kirat-Chatel S, Herman P, Alsteens D, Mahillon J, Hols P, Dufrene YF.** 2013. Single-cell force spectroscopy of probiotic bacteria. Biophys J **104:**1886-1892.

33. **Beaussart A, El-Kirat-Chatel S, Sullan RM, Alsteens D, Herman P, Derclaye S, Dufrene YF.** 2014. Quantifying the forces guiding microbial cell adhesion using single-cell force spectroscopy. Nat Protoc **9:**1049-1055.

34. **Formosa-Dague C, Fu ZH, Feuillie C, Foster TJ, Geoghegan JA, Dufrene YF.** 2016. Forces between *Staphylococcus aureus* and human skin. Nanoscale Horizons **1:**298-303.

35. **Formosa-Dague C, Speziale P, Foster TJ, Geoghegan JA, Dufrene YF.** 2016. Zinc-dependent mechanical properties of *Staphylococcus aureus* biofilm-forming surface protein SasG. Proc Natl Acad Sci U S A **113:**410-415.

36. **Murphy E, Lin SL, Nunez L, Andrew L, Fink PS, Dilts DA, Hoiseth SK, Jansen KU, Anderson AS.** 2011. Challenges for the evaluation of *Staphylococcus aureus* protein based vaccines: monitoring antigenic diversity. Hum Vaccin **7 Suppl:**51-59.

37. **Ganesh VK, Liang X, Geoghegan JA, Cohen AL, Venugopalan N, Foster TJ, Hook M.** 2016. Lessons from the Crystal Structure of the *S. aureus* Surface Protein Clumping Factor A in Complex With Tefibazumab, an Inhibiting Monoclonal Antibody. EBioMedicine doi:10.1016/j.ebiom.2016.09.027.

38. **Kezic S, O'Regan GM, Yau N, Sandilands A, Chen H, Campbell LE, Kroboth K, Watson R, Rowland M, McLean WH, Irvine AD.** 2011. Levels of filaggrin degradation products are influenced by both filaggrin genotype and atopic dermatitis severity. Allergy **66:**934-940.

39. **Pellerin L, Henry J, Hsu CY, Balica S, Jean-Decoster C, Mechin MC, Hansmann B, Rodriguez E, Weindinger S, Schmitt AM, Serre G, Paul C, Simon M.** 2013. Defects of filaggrin-like proteins in both lesional and nonlesional atopic skin. J Allergy Clin Immunol **131:**1094-1102.

40. **Weidenmaier C, Goerke C, Wolz C. 2012**. *Staphylococcus aureus* determinants for nasal colonization. Trends Microbiol 20:243-250.

41. **Rojo A, Aguinaga A, Monecke S, Yuste JR, Gastaminza G, Espana A.** 2014. *Staphylococcus aureus* genomic pattern and atopic dermatitis: may factors other than superantigens be involved? Eur J Clin Microbiol Infect Dis **33:**651-658.

42. **Yeung M, Balma-Mena A, Shear N, Simor A, Pope E, Walsh S, McGavin MJ.** 2011. Identification of major clonal complexes and toxin producing strains among *Staphylococcus aureus* associated with atopic dermatitis. Microbes Infect **13:**189-197.

43. **Harris SR, Cartwright EJ, Torok ME, Holden MT, Brown NM, Ogilvy-Stuart AL, Ellington MJ, Quail MA, Bentley SD, Parkhill J, Peacock SJ.** 2013. Whole-

genome sequencing for analysis of an outbreak of meticillin-resistant *Staphylococcus aureus*: a descriptive study. Lancet Infect Dis **13:**130-136.

622 **Figure Legends**

623 **Fig. 1. Clonal complex assignments of AD strains and control strains of *S. aureus*.**

624 Swabs were taken from a clinically infected site on the AD patient's skin (A, AD strains) or
625 from the anterior nares of asymptomatic carriers (B, control strains). A single colony isolate
626 from each patient was *spa* typed. One or more isolates of each unique *spa* type were
627 subjected to multilocus sequence typing and clonal complex (CC) was assigned by eBURST
628 analysis.

629

630 **Fig. 2. Adherence of *S. aureus* strains to L2v.** Control strains (■) or AD strains (●) were
631 grown to exponential phase, adjusted to an OD_{600} = 1.0 and incubated in wells coated with
632 L2v at 37°C. Following incubation wells were washed, adherent bacteria were stained with
633 crystal violet and the absorbance was read at 570 nm. Each data point represents the mean
634 adherence value of a single strain from three independent experiments expressed as a
635 percentage of the absorbance value measured for strain SH1000. Strains from CC1 are
636 shown in red, CC8 in blue, CC30 in green and other CCs in black. The horizontal lines
637 represent the median adherence value for the population. Statistical analysis was performed
638 using an unpaired *t*-test, *** $p < 0.001$.

639

640 **Fig. 3. Characterisation of a ClfB-deficient mutant of *S. aureus* $AD08_{CC1}$.** A) The *S.*
641 *aureus* strain $AD08_{CC1}$ (1), its isogenic ClfB-deficient mutant $AD08_{CC1}\Delta clfB$ (2) and
642 complemented mutant $AD08_{CC1}\Delta clfB$ (pCU1::*clfB*) (3) were grown to exponential phase.
643 Cell wall extracts were separated on 7.5 % acrylamide gels, blotted onto PVDF membranes
644 and ClfB was detected using polyclonal rabbit antibodies. Bound antibody was detected
645 using horseradish peroxidise-conjugated protein A. Size markers (kDa) are indicated.

B) *S. aureus* strain AD08$_{CC1}$ (●) and AD08$_{CC1}$Δ*clfB* (■) were grown to exponential phase, washed and incubated in microtiter plates coated with L2v. Adherent cells were stained with crystal violet and the absorbance was read at 570 nm. The graph shown is representative of three independent experiments.

C) *S. aureus* strain AD08$_{CC1}$ (red) or mutants AD08$_{CC1}$Δ*clfB* (blue), AD08$_{CC1}$Δ*clfB* (pCU1) (white) and AD08$_{CC1}$Δ*clfB* (pCU1::*clfB*) (green) were grown to exponential phase, washed and incubated in microtiter plates coated with L2v (0.625 µg/ml). Adherent cells were stained with crystal violet and the absorbance was read at 570 nm. Error bars represent the standard error of the mean values obtained from three independent experiments. Statistical significance was determined with Student's unpaired *t*-test, $^{**}P = 0.0059$, $^{***}P < 0.0001$.

Fig. 4. Strength of the *S. aureus*-corneocyte interaction. (a) Box-chart of the adhesion forces recorded between *S. aureus* AD08$_{CC1}$ or *S. aureus* AD08$_{CC1}$Δ*clfB* and corneocytes from patient 1434. (b) Representative force curves recorded in each condition. (c) Box-chart of the adhesion force between *S. aureus* AD08$_{CC1}$ or *S. aureus* AD08$_{CC1}$Δ*clfB* and corneocytes from patient 1473. (d) Representative force curves recorded in each condition. All curves were obtained using an applied force of 250 pN and an approach and retraction speed of 1.0 µm/s. In each case, values calculated from force curves recorded for 5 different *S. aureus*-corneocyte pairs were pooled and represented as box-charts, showing mean adhesion (full circle), median, first and third quartiles (box), range of data without outliers (whiskers), 99th percentile (open circle) and extreme outliers (triangles). Statistical analysis was performed using an unpaired *t*-test, *** $p < 0.0001$.

669 **Fig. 5. Nanoscale multiparametric imaging of corneocytes using single *S. aureus* probes.**
670 (a) Height image of a corneocyte coming from patient 1434 recorded in PBS using a *S.*
671 *aureus* $AD08_{CC1}$ cell probe, and (b) corresponding adhesion image. (c) Height image of a
672 corneocyte coming from patient 1434 recorded in PBS using a *S. aureus* $AD08_{CC1}\Delta clfB$ cell
673 probe, and (d) corresponding adhesion image. For both conditions, similar data were
674 obtained in two other independent experiments.

675

676 **Fig. 6. Binding of rClfB N2N3 to L2v.** A) Ribbon representation of the crystal structure of
677 the N2N3 subdomains of ClfB showing the residues that vary between the CC1 and CC30
678 sequences (red). The ClfB ligand bound in the trench between subdomains N2 and N3 is
679 shown in stick format (blue). Representative sensorgrams showing binding of rClfB N2N3 to
680 L2v in a single cycle kinetics assay. GST-tagged L2v was captured on a CM5 chip coated
681 with anti-GST IgG and increasing concentrations of rClfB N2N3 with the CC1 (B) or CC30
682 (C) sequence were passed over the surface. Binding was plotted as response units against
683 time. The affinities were calculated from curve fitting to a plot of the response unit values
684 against concentrations of rClfB N2N3. The data shown is representative of 3 individual
685 experiments.

686

687

688

689

690

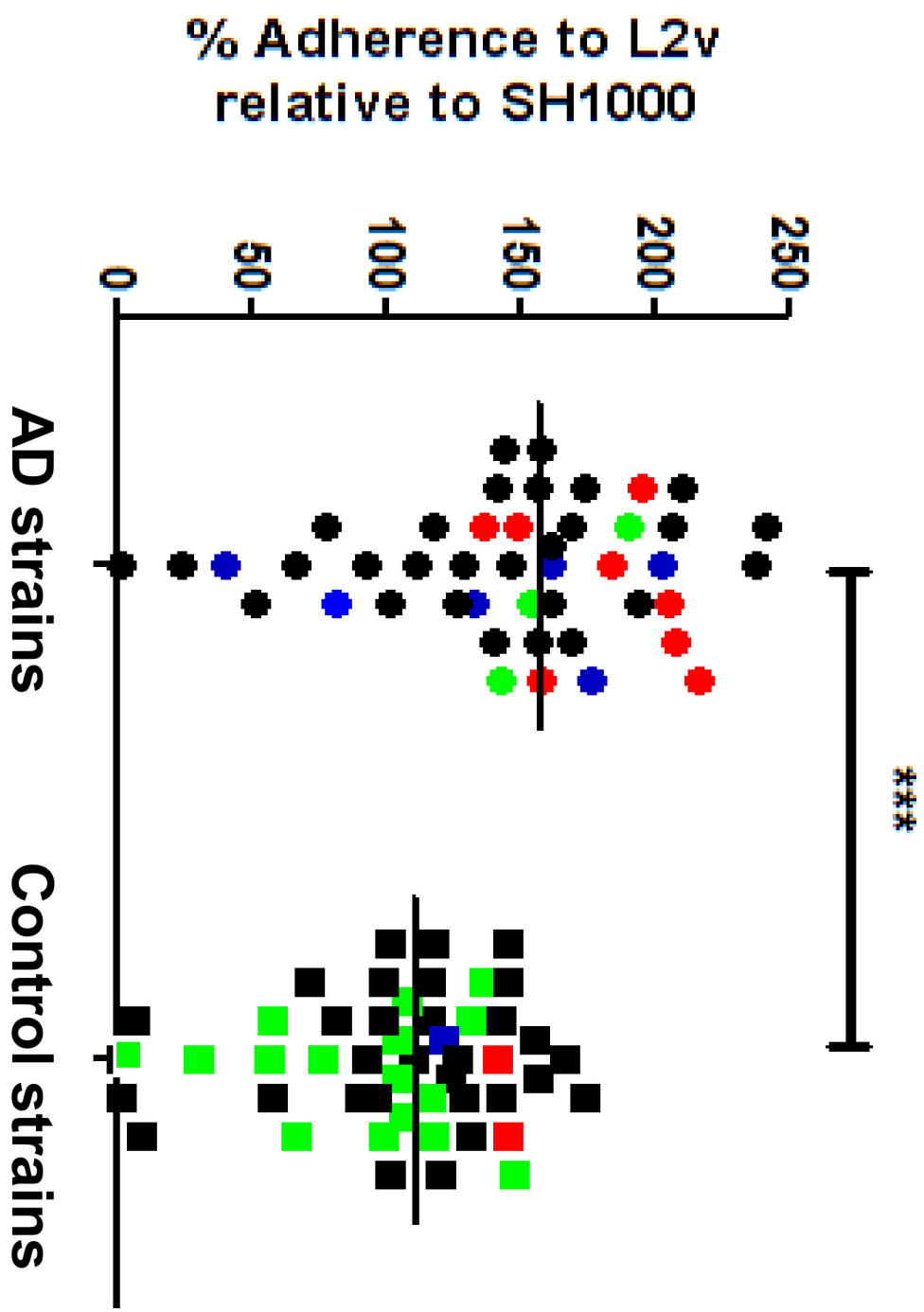

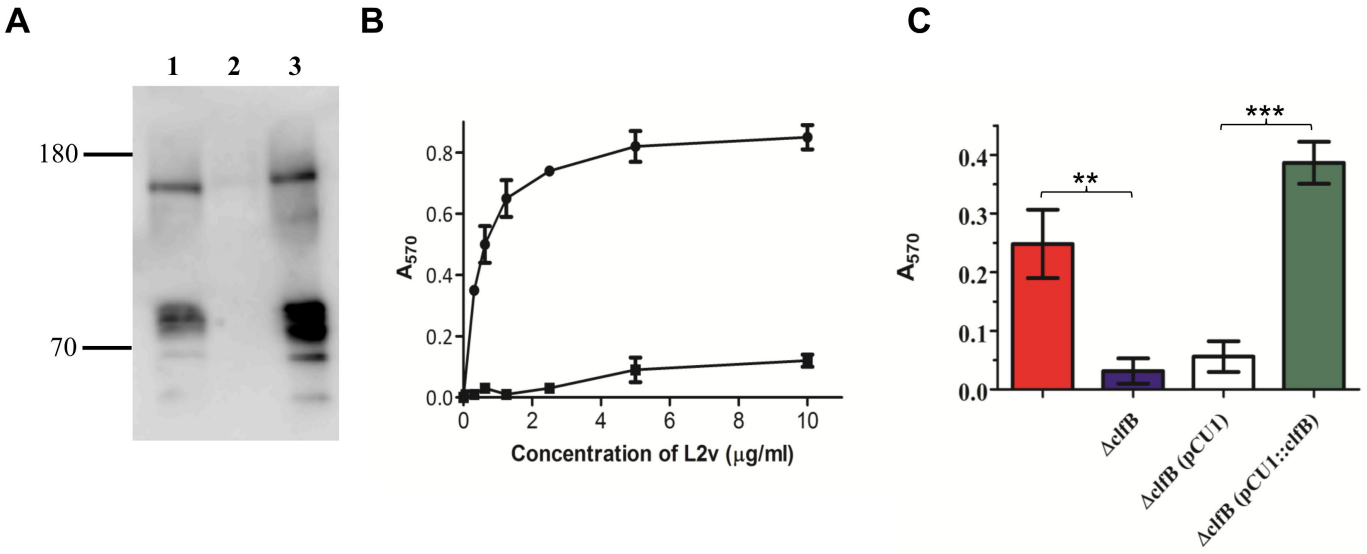

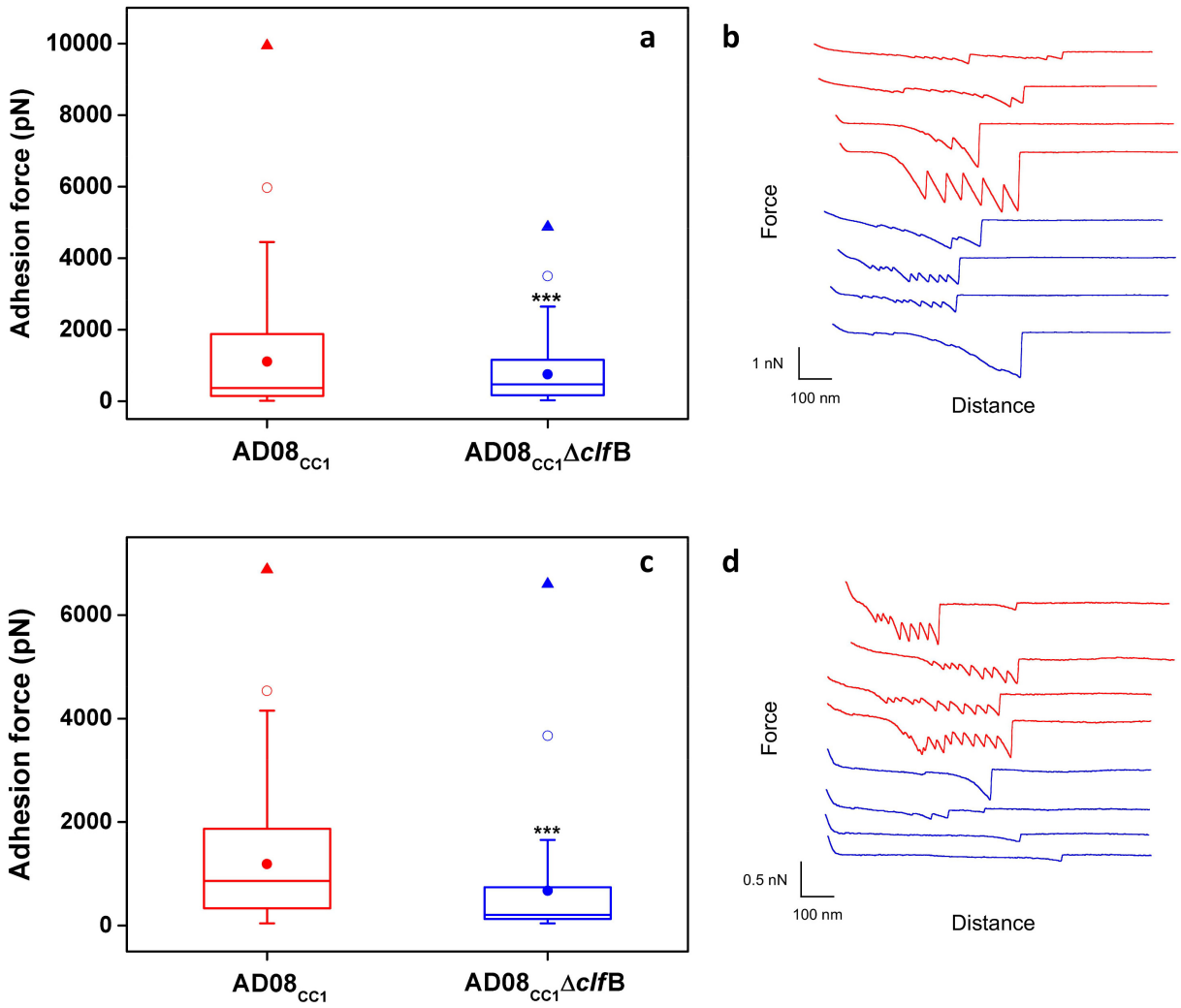

Infection and Immunity